

Published on *Silicates Industriels*, 68 [5-6] (2003) 67-73  
Copyright © 2003 The Belgian Ceramic Research Centre. All rights reserved.

# Effect of talc and chlorite on sintering and technological behaviour of porcelain stoneware tiles

V. Biasini\*, M. Dondi\*, G. Guarini\*, M. Raimondo\*, A. Argnani<sup>§</sup>, S. Di Primio<sup>§</sup>

\* CNR, Istituto di Scienza e Tecnologia dei Materiali Ceramici, via Granarolo 64, I-48018 Faenza (Italy)

<sup>§</sup> Maffei s.p.a., via G. Reni 2/I, I-42014 Castellarano (Italy)

---

## Abstract

The use of magnesium silicates as sintering promoters in porcelain stoneware tiles was investigated in order to understand their effect on technological properties and firing behaviour. Three formulations were designed, replacing sodic feldspar with 3% wt talc or chlorite in a reference porcelain stoneware body, and experimented at a laboratory scale simulating the industrial tilemaking cycle. The occurrence of magnesium silicates does not affect the technological properties of semi-finished products, but it influences remarkably the firing behaviour. Bodies containing talc or chlorite exhibit a faster densification kinetics, with slightly larger firing shrinkages, due to their larger amount of glassy phase, which appears to be less viscous than the reference one. On the other hand, the addition of magnesium silicates brings about a slightly lower bulk density, basically due to a larger amount of closed porosity, being water absorption negligible over 1160°C. Notwithstanding the different porosity, porcelain stoneware bodies containing talc or chlorite present just a moderate decrease of mechanical strength.

---

## 1. Introduction

Porcelain stoneware tiles are products with high technical performances, particularly mechanical, wear and frost resistance, which are to a large extent connected with their very low values of water absorption, around 0.1% [1-4]. In order to achieve this strict porosity requirement, large amounts of fluxes, mainly sodic feldspar, are currently introduced into the porcelain stoneware bodies, promoting the sintering process through the formation during firing of an abundant liquid phase [4-6]. An enhancement of the densification kinetics is often pursued by adding magnesium-bearing raw materials (e.g. talc, dolomite), which should improve the physical properties of the liquid phase, increasing its surface tension and decreasing its viscosity [7].

In this standview, the present study is aimed at outlining the effects of magnesium silicates on technological behaviour and sintering of porcelain stoneware bodies. The rationale of this work is a direct comparison, performed through a laboratory scale simulation of the tilemaking process, of talc- and chlorite-bearing formulations with a reference one.

## 2. Experimental

Three different formulations were designed on the basis of the current experiences in the tilemaking industry: a typical formulation for porcelain stoneware tiles (G1) and two alternative bodies, one containing talc (G2) and the other a chlorite-bearing sodic feldspar (G3) in replacement of a conventional feldspathic flux. These amounts of talc and chlorite were designed to provide 1% MgO, with limited changes in the other oxides (Table 1).

These bodies underwent a simulation of the industrial tilemaking manufacture: dry mixing of raw materials, wet grinding in porcelain jar with dense alumina grinding media (18 h), slip drying in oven ( $100 \pm 5$  °C), powder deagglomeration by hammer milling (grid 0.75 mm), powder humidification and pelletizing, unidirectional pressing of 110-55-6 mm<sup>3</sup> tiles (40 MPa), drying in oven ( $100 \pm 5$  °C), firing in a laboratory electric roller kiln (maximum temperature 1120-1180 °C, cycle 60 minues cold-to-c old).

The semi-finished products were characterised measuring:

- weight volume and water content of slips (gravimetric method);
- particle size distribution (ASTM C 958), working moisture (ASTM C 324) and compressibility (mould depth/tile thickness ratio) of powders;
- pressing expansion and drying shrinkage (ASTM C 326);
- green and dry modulus of rupture (ISO 10545-4).
- The fired tiles were characterised determining:
  - firing shrinkage (ASTM C 326);
  - water absorption, open porosity and bulk density (ISO 10545-3);
  - total porosity, as ratio between bulk density and specific weight of ceramic material (ASTM C 329), and closed porosity by difference;
  - modulus of rupture (ISO 10545-4);
  - microstructure by scanning electron microscope (Cambridge Stereoscan 360) observations on lapped surfaces;
  - quantitative phase composition by X-ray powder diffraction (Rigaku Miniflex, Ni-filtered CuK $\alpha$  radiation) with RIR method using CaF<sub>2</sub> as internal standard;
  - bulk chemical composition of tiles by ICP-OES (Varian Liberty 200, alkaline fusion in graphite crucible);
  - chemical composition of the glassy phase, calculated on the basis of phase composition and bulk chemistry of tiles;
  - surface tension and viscosity of the liquid phase at sintering temperatures, estimated on the basis of the chemical composition of the glassy phase, respectively with Cambier and Leriche [7] and Deletter et al. [8] methods;
  - kinetic parameter K', calculated on the basis of thermodilatometric analysis (Netzsch STA 1400) in isothermal conditions (1000, 1050 and 1100 °C) according to the equation [9]:

$$\text{Log } K' = (1/m) \cdot \text{Log } (\Delta L/L_0) - \text{Log } t + \text{Log } T$$

where m is the slope of the straight line in the bilogarithmic diagram time vs shrinkage,  $\Delta L/L_0$  is the linear shrinkage, t is the time (min) and T is the temperature (°K).

### 3. Results And Discussion

#### 3.1. Semi-finished products

The particle size distribution of the three bodies is practically the same and it corresponds to a typical granulometry of industrially manufactured porcelain stoneware bodies (Fig. 1). The characteristics of slips, powders, green and dry tiles are substantially equivalent in all samples, being the small differences of mechanical strength basically attributable to a slightly lower working moisture of body G2 in respect of the other mixtures (Table 2).

#### 3.2. Densification process

The experimental bodies behave in a different way during the firing process (Fig. 2 and Table 3). In particular, the mixes containing magnesium silicates exhibit both higher linear

shrinkage and bulk density as well as lower water absorption up to 1160 °C, while at 1180 °C all values are close each other.

The total porosity of the body G1 decreased rapidly in the 1120-1160 °C range, stabilising at 1180 °C on low percentages (2-3%). In contrast, the addition of magnesium silicates promoted a smoother trend, with a slower but constant diminution of porosity. This tendency is due to a large extent to the persistence in the talc- or chlorite-bearing mixes of a significant amount of closed porosity (5-6%), while in the reference body an abrupt decrease to a minimum around 1% occurred in the 1140-1160 °C range, followed by a moderate increase up to 1180 °C.

On the whole, the three bodies are characterised by similar gradients of linear shrinkage and water absorption in function of firing temperature (Fig. 2). However, body G1 appears to be less reactive than G2 or G3, whose curves are shifted of about 20 °C toward lower temperatures. This 'advantage' in the densification process showed by bodies containing magnesium silicates is accomplished early in the firing and not at the maximum temperatures. As a matter of fact, the gap between G1 on one side and G2 or G3 on the other side is evident already at 1120 °C.

The sodic body G1 is able to reduce efficaciously its porosity, and the closed one in particular, while the sodic-magnesian formulations G2 and G3 retain a significant amount of closed pores. This circumstance could be connected with the variable composition of the glassy phase, with special concern to a different gas solubility.

### 3.3. Phase composition

The phase composition of the experimented porcelain stoneware tiles consists essentially of quartz, plagioclase, mullite and glassy phase (Fig. 3).

Residual quartz after firing at 1180 °C was found in similar amounts in all samples. Nevertheless, there are different rates of solubilisation, since quartz contents at 1120 °C are noteworthy different in the three bodies. Plagioclase melted rapidly passing from amounts of 14-16% (1120 °C) to less than 7% (1180 °C). This dissolution process appears to be faster in talc- and chlorite-bearing mixes, particularly in the 1140-1160 °C range. Mullite is quite constant (8-12%) in the entire thermal range investigated, with a vague trend: the higher the firing temperature, the slightly larger the quantity of mullite. The amount of glassy phase increased apparently with the same rate in all bodies, though it is clearly more abundant in the formulations containing magnesium silicates.

### 3.4. Microstructure

A comparison among fully sintered tiles was performed on samples with water absorption as low as 0.1%. Microstructural observations basically confirmed the porosity measurements: bodies G2 and G3 exhibit a larger residual porosity with respect to mix G1 (Fig. 4).

These pores pertain to several typologies and they have different origins:

- cavities at the boundary of relatively coarse grains, mostly consisting of quartz crystals (Fig. 5A). The occurrence of such pores, up to 10 µm in diameter, may be attributed to two distinct and converging processes: i) pore concentration at the grain boundary during the early stages of sintering, and ii) abrupt volume decrease during cooling due to the  $\beta$ -quartz  $\rightarrow$   $\alpha$ -quartz polymorph transformation.
- Spherical pores enclosed into vitrified zones of the ceramic body (Fig. 5B). The formation of these holes, generally below 10 µm in diameter, is basically connected with the presence of gas into the pores, which may be: i) entrapped by the strong thermal gradient of fast firing, and/or ii) released by the glassy phase while its composition changed with temperature.

- Cavities of size around 10-50  $\mu\text{m}$  and irregular shape (Fig. 5C) which may presumably be the result of manufacturing defects (particle size dishomogeneities, pressing laminations, etc.) and/or coalescence of two or more smaller pores.

### 3.5. Mechanical properties

Bending strength depends on firing temperature, but clearly distinct trends were detected in the reference body and the mixes containing talc or chlorite (Fig. 6). In fact, the modulus of rupture of body G1 increased regularly with temperature and it stabilised around 51 MPa in the fully sintered tiles. In contrast, the increment of bending strength in bodies G2 and G3 occurred only up to 1140 °C, then the modulus of rupture progressively diminished, notwithstanding the total porosity tends to decrease down to 5-7%.

Since the values of the modulus of rupture cannot be justified by the porosity alone, an important role is probably played by the amount of glassy phase and by the size distribution of pores and microstructural defects.

### 3.6. Composition and viscosity of the liquid phase

The chemical composition of the glassy phase changed with firing temperature, according to different trends (Table 4). For increasing temperatures, body G1 showed an augment of silica together with a decrease of alumina and potassium oxide, while sodium oxide appears to be quite constant. On the contrary, the glassy phase of bodies G2 and G3 is characterised by relatively high magnesium content, rather constant values of silica, a diminution of alumina and potassium oxide as well as an increase of sodium and calcium oxides (Fig. 7).

These chemical variations have strong repercussions on the physical properties of the liquid phase at sintering temperatures, particularly viscosity and surface tension (Table 4). As a matter of fact, the liquid phase of bodies G2 and G3 is less viscous and exhibits a slightly higher surface tension, due probably to both larger amount of alkaline-earth oxides and lower percentage of silica in respect of body G1.

### 3.7. Sintering kinetics

The densification of the experimental bodies in isothermal conditions confirmed the results of technological testing: firing shrinkage is larger in magnesium-rich mixtures (Fig. 8).

The slope of the 'linear shrinkage versus time' curves is similar for bodies G1 and G2, but it is significantly steeper in the case of mix G3. This circumstance suggests that sintering occurred initially with a faster rate in presence of magnesium silicates, and that chlorite is more effective than talc.

This observation is enhanced by the adimensional kinetic parameter  $K'$  [9], which is neatly larger in body G3 (3.1) in respect of bodies G2 and G1 (1.7 and 0.4 respectively).

## 4. Conclusions

The introduction of talc or chlorite in porcelain stoneware bodies has no relevant influence on the characteristics of semi-finished products (slips, powders, green and dry tiles), but it determines a significant change in technological behaviour during the firing process.

The effect of talc or chlorite can be highlighted comparing porcelain stoneware tiles having suitable values of water absorption (i.e. 0.1%). In this case, the presence of magnesium silicates promotes some significant changes of firing behaviour (Table 5):

- a greater reactivity, permitting lower firing temperatures (of about 20 °C) to achieve the same water absorption;

- a larger amount of residual porosity, mostly represented by closed pores;
- a slightly lower bulk density;
- a limited increase of firing shrinkage;
- a moderate decrease of bending strength.

The enhanced reactivity of bodies containing talc or chlorite is justified by the larger amount and the different composition of the liquid phase formed during firing. In effect, the glassy phase is considerably more abundant in bodies G2 and G3, where it contains more MgO and CaO, less silica, and similar amounts of alkalis. These features contribute to lower its viscosity and to increase slightly its surface tension, so improving the sintering kinetics.

The larger amounts of closed porosity persisting in the tiles containing magnesium silicates is presumably connected with:

- a faster densification kinetics, which may promote an entrapment of gas bubbles due to an abrupt decrease of permeability;
- a release of gas bubbles from the liquid phase, due to a change of gas solubility consequent to a variation in composition of the glass.

The different mechanical properties are attributable to a large extent to the variable porosity of porcelain stoneware tiles. However, the bodies with magnesium silicates exhibit a complex behaviour, which is probably connected with a different microstructure, especially for what concerns a size distribution of pores and defects.

## References

- [1] L. Barbieri, L. Bonfatti, A.M. Ferrari, C. Leonelli, T. Manfredini and D. Settembre Blundo, Relationship between microstructure and mechanical properties in fully vitrified stoneware, Proc. 8<sup>th</sup> CIMTEC, World Ceramic Congress, Firenze 1994.
- [2] M. Dondi, B. Fabbri, T. Manfredini and G.C. Pellacani, Microstructure and mechanical properties of porcelainized stoneware tiles, 4th Euro-Ceramics, 11 (1995) "Floor and Wall Tiles", C. Palmonari (ed.), Faenza Ed., 319-326.
- [3] T. Manfredini, G.C. Pellacani, M. Romagnoli and L. Pennisi, Porcelainized stoneware tile, Am. Ceram. Soc. Bull., 75 (1995) [5] 76-79.
- [4] M. Dondi, G. Ercolani, M. Marsigli, C. Melandri and C. Mingazzini, The chemical composition of porcelain stoneware tiles and its influence on microstructure and mechanical properties. Interceram, 48 [2] (1999) 75-83.
- [5] M.J. Orts, A. Escardino, J.L. Amorós and F. Negre, Microstructural changes during the firing of stoneware floor tiles. Applied Clay Science, 8 (1993) 193-205.
- [6] G. Biffi, Porcelain stoneware. Gruppo Editoriale Faenza Editrice (1996) Faenza.
- [7] F. Cambier and A. Leriche, Vitrification. In: R.W. Cahn, P. Haasen, E.J. Kramer (eds.), "Materials Science and Technology, A Comprehensive Treatment", vol. 17B, Processing of Ceramics, Part II, VCH () 123-144.
- [8] M. Deletter, F. Cambier, M.R. Anseau, I. N'Dala and G. Urbain, Viscosity of liquid feldspars – Part II: Model for estimating the viscosities of feldspar type melts. Br. Ceram. Trans., 83 (1984) 108-112.
- [9] V.K. Singh, Sintering of calcium aluminate mixes. Br. Ceram. Trans., 98 [4] (1999) 187-191.

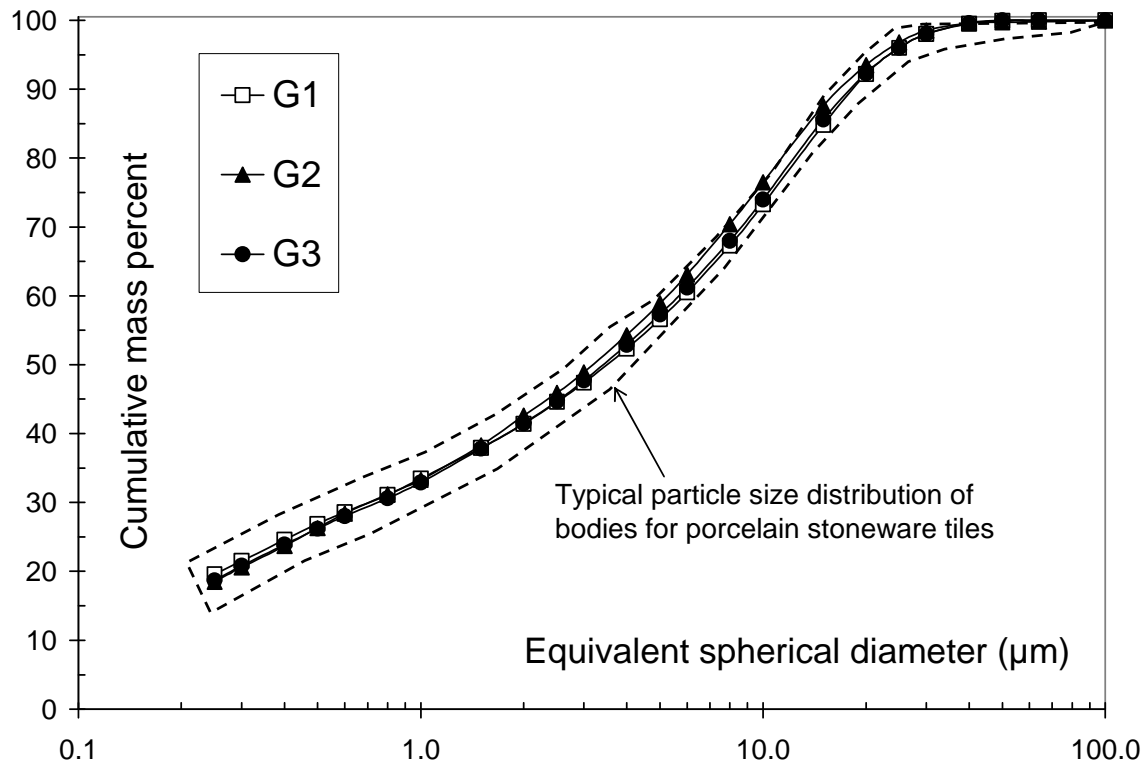


Figure 1. Particle size distribution of the wet ground porcelain stoneware bodies.

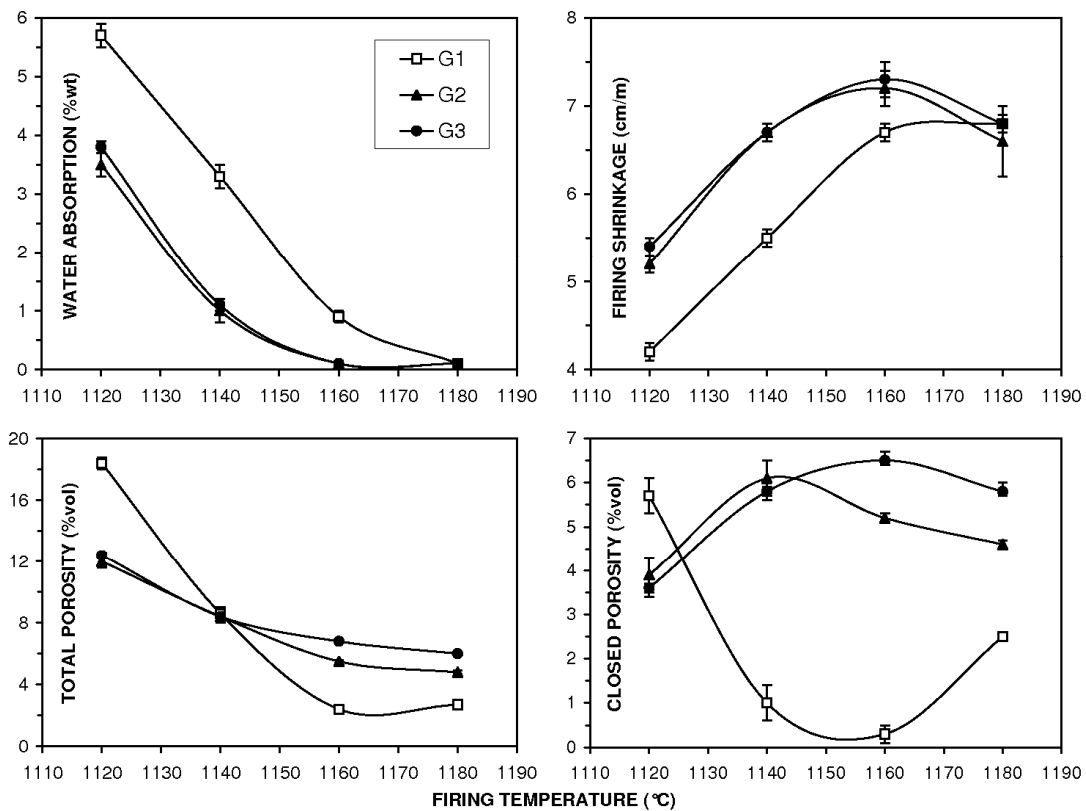


Figure 2. Firing behaviour of the experimental bodies.

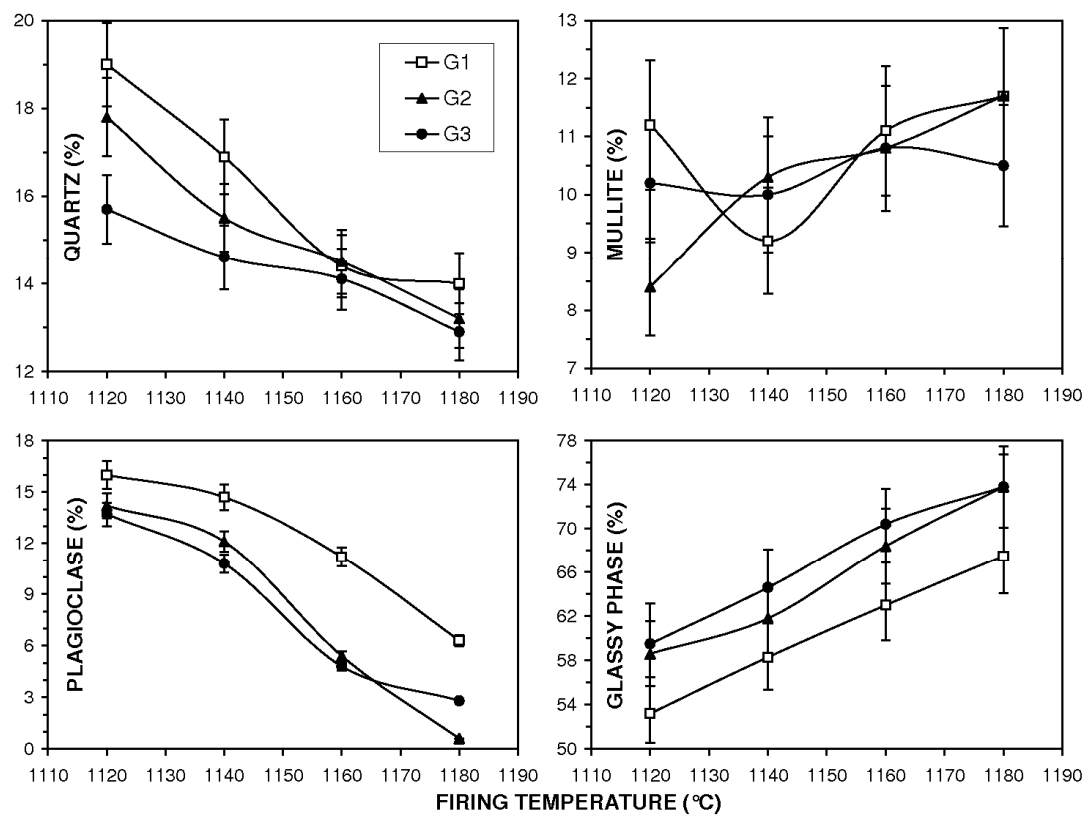


Figure 3. Phase composition of the experimental bodies.

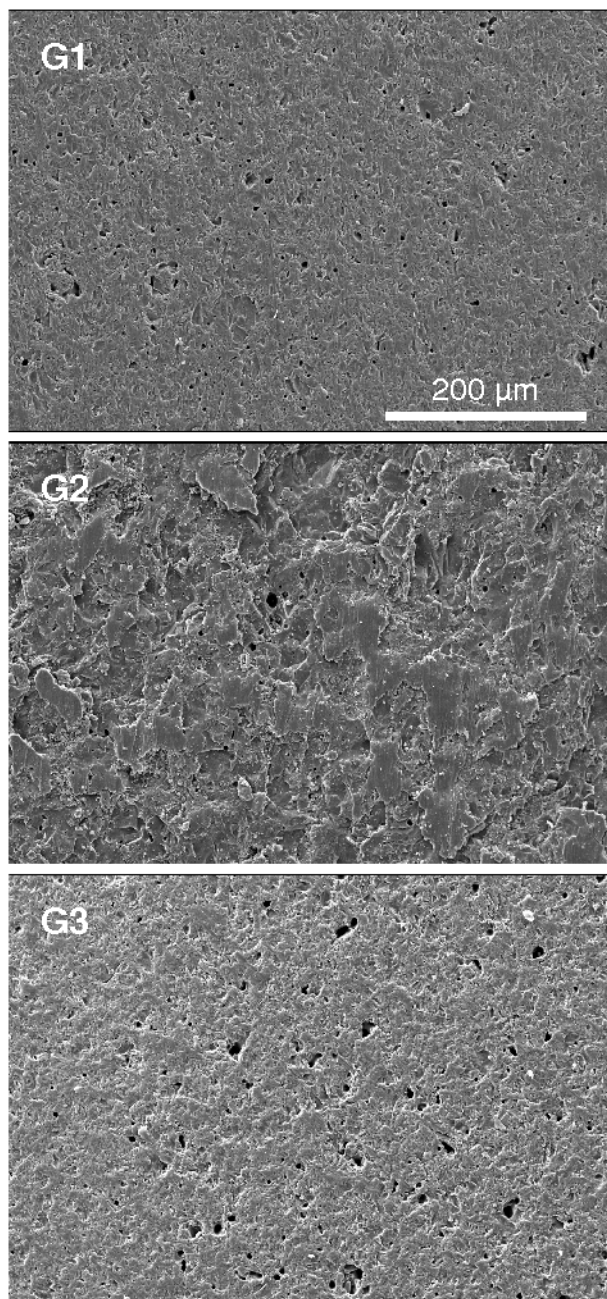


Figure 4. SEM photomicrographs of the lapped surface of bodies fired at 1180 °C (G1) or 1160 °C (G2 and G3).



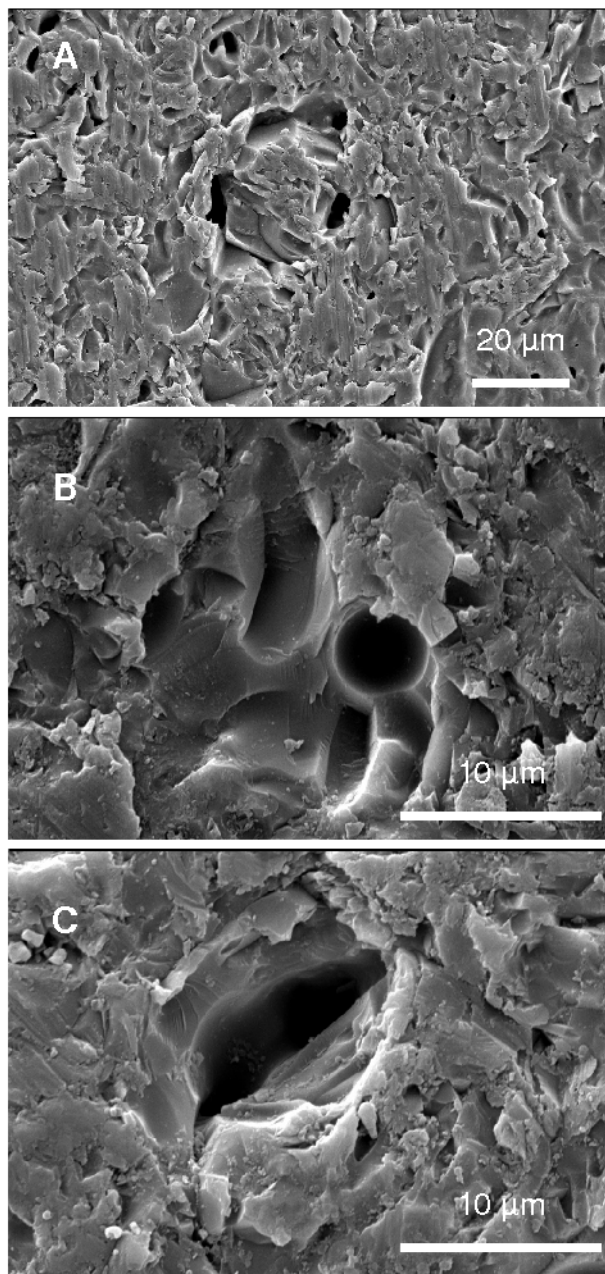


Figure 5. SEM photomicrographs of different types of pores found in fired bodies. A) cavities at the boundary of coarse grains; B) bubble into the glassy phase; C) pore with irregular shape in contact with the glassy phase.

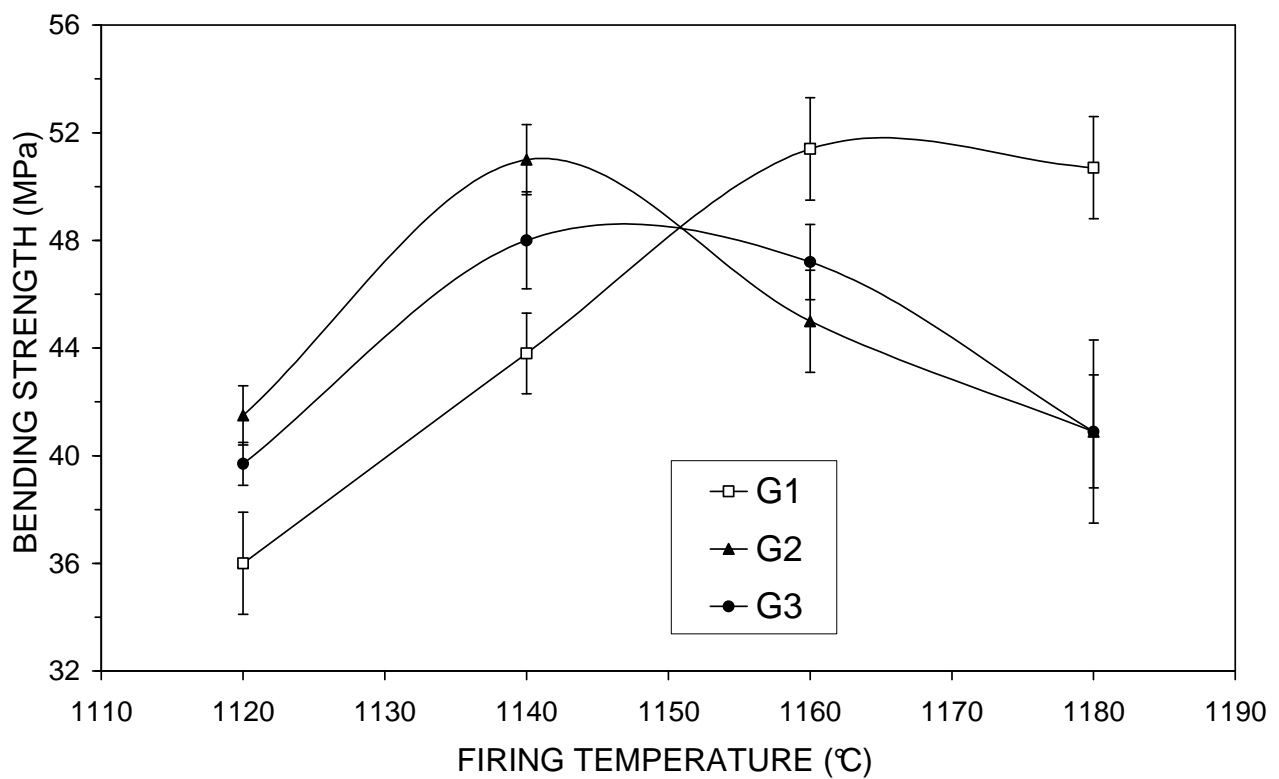


Figure 6. Modulus of rupture of the experimental bodies in function of firing temperature.

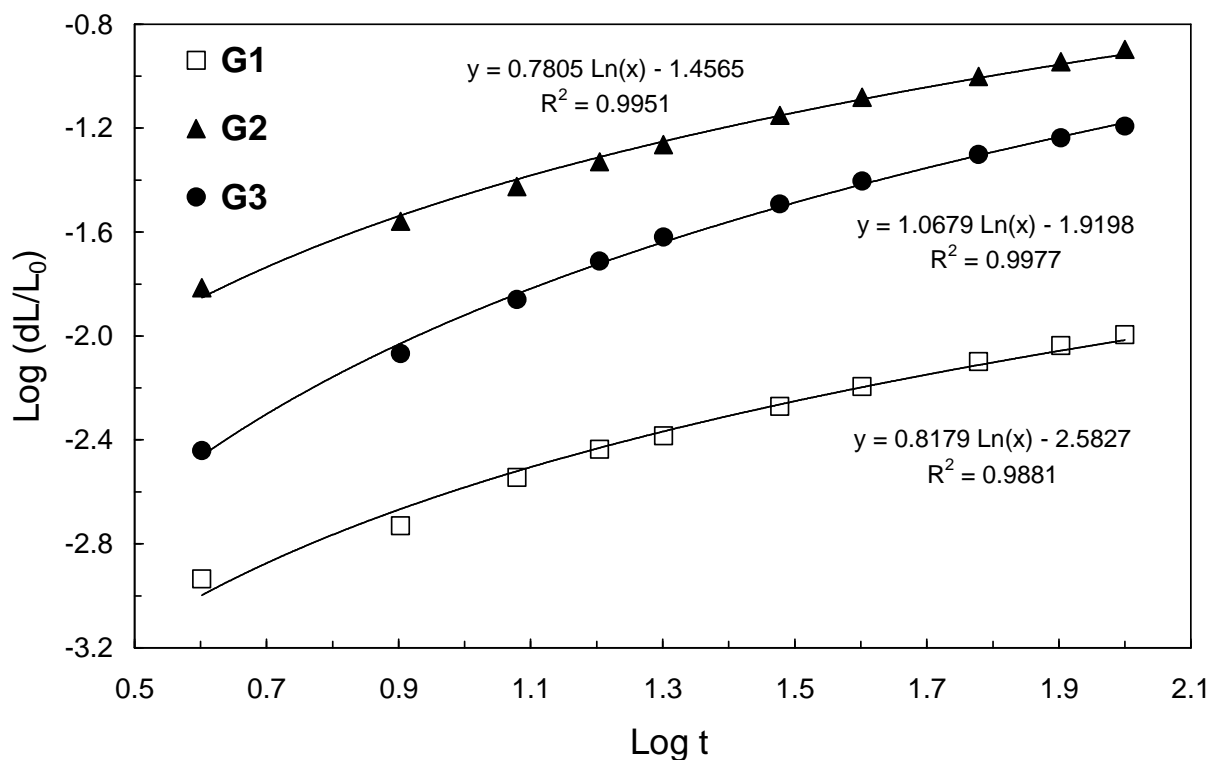


Figure 8. Bilogarithmic diagram (linear shrinkage vs time) of isothermal DTA data (1100 °C) of the experimental bodies

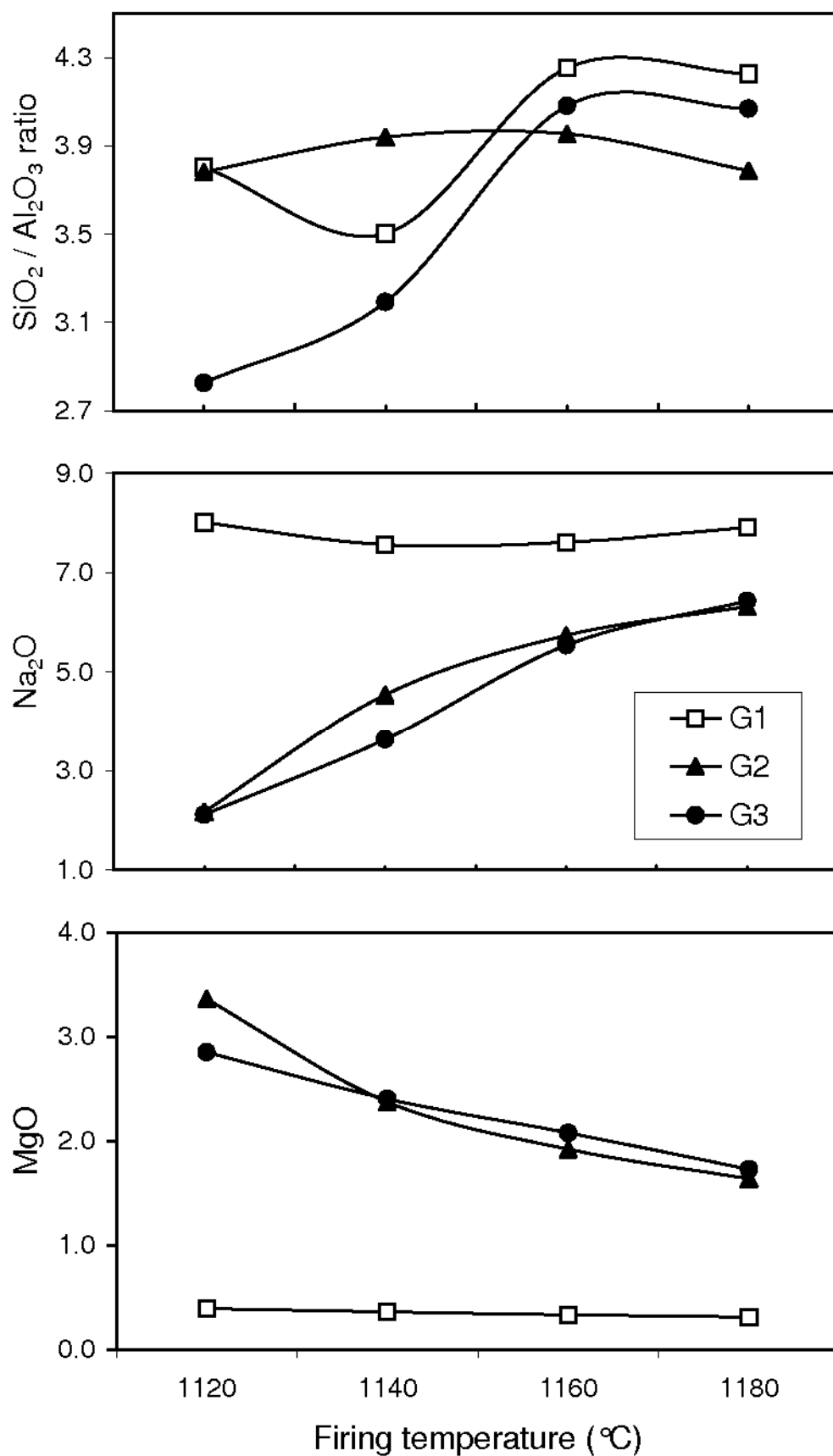


Figure 7. Chemical composition of the glassy phase in function of firing temperature.

Table 1  
 Formulation and chemical composition of the experimental bodies

Raw material (% weight)	Body G1	Body G2	Body G3
Ball clay (Ukraine)	20	20	20
Ball clay (Westerwald)	15	15	15
Quartz sand (Sardinia)	15	15	12
<b>Sodic feldspar (Turkey)</b>	50	47	20
Talc (Spain)	0	3	0
Chlorite-bearing sodic feldspar (Sardinia)	0	0	33
SiO <sub>2</sub>	67.1	66.8	65.9
TiO <sub>2</sub>	0.6	0.6	0.7
Al <sub>2</sub> O <sub>3</sub>	20.6	20.2	20.7
Fe <sub>2</sub> O <sub>3</sub>	0.4	0.5	0.6
MgO	0.2	1.2	1.2
CaO	0.4	0.4	0.7
Na <sub>2</sub> O	5.8	5.4	5.2
K <sub>2</sub> O	1.8	1.8	1.7
L.o.I.	3.0	3.2	3.4

Table 2  
 Technological properties of semi-finished products

Property	Unit	Body G1	Body G2	Body G3
Water content of slip	<b>cg·g<sup>-1</sup></b>	35.7±0.2	35.1±0.2	35.6±0.2
Specific weight of slip	g·L <sup>-1</sup>	1685±10	1667±10	1665±10
Working moisture of powder	cg·g <sup>-1</sup>	6.1±0.2	5.3±0.2	6.0±0.2
<b>Pressing expansion</b>	cm·m <sup>-1</sup>	0.70±0.05	0.70±0.05	0.64±0.00
Green modulus of rupture	MPa	1.24±0.17	1.10±0.13	1.33±0.24
Compressibility index	adim.	2.9±0.1	3.2±0.1	3.3±0.1
Drying shrinkage	cm·m <sup>-1</sup>	-0.02±0.05	-0.02±0.05	-0.07±0.05
Dry modulus of rupture	MPa	2.43±0.34	2.12±0.35	2.32±0.31

Table 5  
 Comparison of technological performances of ceramic tiles (water absorption <0.2%)

Technological property	Unit	Bodies		
		G1	G2	G3
Maximum firing temperature	°C	1180	1160	1160
Water absorption	% wt.	0.1	0.1	0.1
Total porosity	% vol.	2.7	5.5	6.8
Open porosity	% vol.	0.2	0.3	0.3
Closed porosity	% vol.	2.5	5.2	6.5
Bulk density	g·cm <sup>-3</sup>	2.48	2.43	2.43
Firing shrinkage	cm·m <sup>-1</sup>	6.8	7.2	7.3
Bending strength	MPa	50.7	45.0	47.2

**Table 3**  
 Technological properties of ceramic tiles

Property	Unit	BODY G1				BODY G2				BODY G3			
		1120°C	1140°C	1160°C	1180°C	1120°C	1140°C	1160°C	1180°C	1120°C	1140°C	1160°C	1180°C
Firing shrinkage	cm·m <sup>-1</sup>	4.2±0.1	5.5±0.0	6.7±0.1	6.8±0.1	5.2±0.1	6.7±0.1	7.2±0.2	6.6±0.4	5.4±0.1	6.7±0.1	7.3±0.2	6.8±0.1
Water absorption	% wt.	5.7±0.2	3.3±0.2	0.9±0.1	0.1±0.05	3.5±0.2	1.0±0.2	0.1±0.05	0.1±0.05	3.8±0.1	1.1±0.1	0.1±0.0	0.1±0.0
Total porosity	% vol.	18.4±0.4	8.6±0.4	2.4±0.2	2.7±0.1	12.0±0.4	8.4±0.4	5.5±0.1	4.8±0.1	12.4±0.2	8.4±0.2	6.8±0.1	6.0±0.1
Open porosity	% vol.	12.7±0.4	7.6±0.4	2.1±0.2	0.2±0.1	8.1±0.4	2.3±0.4	0.3±0.1	0.3±0.1	8.7±0.2	2.6±0.2	0.3±0.1	0.2±0.1
Closed porosity	% vol.	5.7±0.4	1.0±0.4	0.3±0.2	2.5±0.1	3.9±0.4	6.1±0.4	5.2±0.1	4.6±0.1	3.6±0.2	5.8±0.2	6.5±0.1	5.8±0.1
Bulk density	g·cm <sup>-3</sup>	2.21±0.01	2.30±0.01	2.38±0.01	2.41±0.01	2.29±0.01	2.39±0.01	2.43±0.01	2.40±0.02	2.28±0.01	2.39±0.01	2.43±0.01	2.38±0.00
Specific weight	g·cm <sup>-3</sup>	2.71±0.01	2.52±0.01	2.44±0.01	2.48±0.01	2.60±0.01	2.61±0.01	2.57±0.01	2.52±0.01	2.61±0.01	2.61±0.01	2.61±0.01	2.54±0.01
Bending strength	MPa	36.0±1.9	43.8±1.5	51.4±1.9	50.7±1.9	41.5±1.1	51.0±1.3	45.0±1.9	40.9±3.4	39.7±0.8	48.0±1.8	47.2±1.4	40.9±2.1

Table 4

**Calculated chemical composition, viscosity ( $\mu$ ) and surface tension ( $\Gamma$ ) of the glassy phase in ceramic tiles**

% wt	BODY G1				BODY G2				BODY G3			
	1120°C	1140°C	1160°C	1180°C	1120°C	1140°C	1160°C	1180°C	1120°C	1140°C	1160°C	1180°C
SiO <sub>2</sub>	68.9	68.5	71.3	71.2	67.0	69.2	70.1	70.7	68.4	68.7	69.2	69.5
Al <sub>2</sub> O <sub>3</sub>	18.1	19.6	16.7	16.8	19.8	17.7	17.0	16.4	18.5	18.4	17.9	17.9
Fe <sub>2</sub> O <sub>3</sub>	0.8	0.7	0.7	0.6	0.8	0.8	0.7	0.7	1.0	0.9	0.8	0.8
MgO	0.4	0.4	0.3	0.3	2.1	2.0	1.8	1.7	2.1	1.9	1.8	1.7
CaO	0.4	0.4	0.4	0.5	0.4	0.4	0.5	0.6	0.6	0.7	0.8	0.9
Na <sub>2</sub> O	8.0	7.6	7.6	7.9	7.0	7.0	7.4	7.6	6.7	6.7	7.0	7.0
K <sub>2</sub> O	3.4	3.0	2.9	2.7	2.9	2.9	2.5	2.4	2.7	2.7	2.5	2.4
$\mu$ (MPa·s)	15.0	8.4	7.2	4.2	4.7	4.1	2.8	2.0	5.2	3.6	2.3	1.6
$\Gamma$ (N·m <sup>-1</sup> )	0.373	0.376	0.371	0.372	0.384	0.379	0.378	0.376	0.382	0.381	0.380	0.380